Multiple scattering of classical waves in systems with liquidlike correlations: Analytical and numerical results for isotropic scatterers

C. J. Walden*
Faculty of Mathematical Studies, University of Southampton, Southampton SO17 1BJ, United Kingdom
(Received 2 September 1997)

By exploiting the analogy between multiple-scattering theory and the Ornstein-Zernike equation of liquid-state theory an analytical solution to the effective medium approximation is obtained in the case of isotropic scatterers, using a simple model pair-correlation function $g(R)$. Results are presented for model scatterers the diameter d of which may be changed without simultaneously altering the scattering strength. Specifically, d is selected to produce a scattering efficiency close to that observed for a Mie scatterer, and the effect of increasing the packing fraction η considered. Numerical results are then presented for more realistic forms of $g(R)$, and possible extensions to the effective medium approximation which incorporate recurrent scattering processes discussed. [S1063-651X(98)07002-0]

PACS number(s): 42.25.Bs, 78.20.Ci, 61.20.−p

I. INTRODUCTION

The study of waves in random media has attracted much attention recently, stimulated in part by the prospects of achieving a classical analog of Anderson localization [1–3]. The search for this effect is of particular interest due to the absence of competing mechanisms of the kind found in its electronic counterpart [4,5].

In selecting candidate systems, one is led, on the basis of the independent scatterer approximation [6], to consider scatterers at or near resonance. At a frequency ω the most naïve Ioffe-Regel criterion [7] $kl_s \lesssim 1$, with $k=\omega/c_0$, c_0 being the phase velocity in the host medium and $l_s \approx (\rho\sigma_s)^{-1}$ the scattering mean free path, then predicts localization for sufficiently high number densities ρ. In principle, of course, l_s contains no information about localization, and more rigorous criteria arise from an examination of l_{tr}, the transport mean free path [8].

Even if we content ourselves with a calculation of l_s or the extinction mean free path l_e, to which it is equivalent in the absence of absorption, there are two problems with the above independent-scattering argument. The first concerns the fact that a resonant scatterer exhibits a scattering cross section σ_s substantially larger than its geometrical cross section πa^2. Therefore dependent-scattering corrections [9] become necessary, since the *optical* volumes of the scatterers begin to overlap at rather modest number densities. The second difficulty is that as ρ is increased it becomes important to account for correlations in the positions of the scatterers.

In the weak scattering regime this latter effect is relatively easy to incorporate. For example, Saulnier *et al.* [10] have considered correlation corrections to independent scattering for a suspension of latex spheres in water, and obtained good agreement with experiment for both the extinction (l_e) and transport (l_{tr}) mean free paths. On the other hand, for strong scatterers such as the titanium dioxide (TiO_2) dispersions studied by van der Mark *et al.* [11] it is difficult to disentangle the effects of correlations from those of dependent scattering.

Of course, if the scatterers are sufficiently strong, one may approach a localization threshold at a volume fraction for which correlations can be safely neglected. Analysis in this regime has been very successfully achieved using a point scatterer model by van Tiggelen and co-workers [8,12–14]. They point out that an argument of the Ioffe-Regel type is better phrased in terms of $\gamma \equiv p_0 l_s$, where $p_0/k = n_{\mathrm{eff}}$ the effective refractive index of the scatterer-filled medium. Their findings suggest that the effects of dependent scattering are always sufficient to maintain γ above the localization threshold. In fact, by considering l_{tr}, they show that this threshold is more accurately located at $\gamma = \gamma_c = 0.972$, at least for isotropic (and uncorrelated) scatterers.

However, since resonant dielectric scatterers typically exhibit scattering efficiencies $Q_s \equiv \sigma_s/\pi a^2$ of between 5 and 10, it is of interest to consider the effect of introducing positional correlations into this model. To this end, we imagine each model scatterer to be embedded within a physically impenetrable (but optically inert) sphere. A similar approach has been adopted by van Tiggelen and Lagendijk [15]. Their analysis is exact to second order in ρ, and is capable of yielding both scattering and transport properties. However, they are restricted to modest packing fractions η. In this paper we employ a different approach, which, while not exact to any given order in ρ, does allow us to study the behavior at large η.

Our calculations focus on the determination of l_s rather than l_{tr}, the latter being considerably more difficult to obtain when correlations are present. Hence, we may obtain a Ioffe-Regel number γ, but have less confidence in locating a localization threshold. Nevertheless, the results are instructive, as they suggest regimes worthy of further investigation.

The starting point for any such calculation is the (ensemble-averaged) amplitude Green function. To determine this exactly requires specification of all the correlation functions that are necessary to fully characterize the random medium. In practice only the pair-correlation function $g(R)$

*Present address: Department of Mathematics, University of Essex, Wivenhoe Park, Colchester CO4 3SQ, U.K.

[16] is available, and one has to resort to approximate theories, such as the well-known quasicrystalline (QCA) [17] and effective medium (EMA) [18] approximations.

A previous paper [19] (hereinafter referred to as I) concerned the formal manipulation of the multiple-scattering theory for scalar waves in a discrete random medium exhibiting liquidlike correlations. It was demonstrated that a one-to-one correspondence exists between that formalism and the Ornstein-Zernike (OZ) equation of liquid-state theory [16]. This leads to a natural distinction between a *direct* $[C(R)]$ and a *total* $[H(R)]$ propagator, the former being identified with what is sometimes termed the medium propagator [18]. A number of existing theories may then be viewed as closure approximations to this integral equation.

The results presented in this paper were derived using this formalism. Section II provides a brief review of the key formulas, restricting attention to isotropic scatterers. Section III concerns the so-called hole-correction (HC) approximation, for which the pair-correlation function is modeled by a step function. In this case we may determine the direct propagator for the EMA in closed form. We employ a method based on the factorization scheme of Baxter [20] to determine $C(R)$ self-consistently. For hard-sphere packing fractions $\eta > 1/8$ the HC model does not correspond to any physically attainable arrangement of scatterers. In this regime we require a better description of the correlation structure. In Sec. IV we present results obtained using a more realistic $g(R)$. Finally, in Sec. V we discuss the limitations of the present approach and suggest extensions which incorporate repeated scattering processes omitted in this treatment.

II. MULTIPLE-SCATTERING THEORY FOR ISOTROPIC SCATTERERS

We now provide a brief outline of the OZ formalism presented in I.

It is convenient to introduce the medium path operator of Roth [18],

$$\hat{\tau}(\mathbf{R}-\mathbf{R}') = \left\langle \sum_{\alpha\beta} \delta(\mathbf{R}-\mathbf{R}_\alpha)\mathcal{T}_{\alpha\beta}\delta(\mathbf{R}'-\mathbf{R}_\beta) \right\rangle, \tag{1}$$

in terms of which the (ensemble-averaged) total T matrix of the system is

$$\hat{T} \equiv \langle \hat{\mathcal{T}} \rangle = \int \hat{\tau}(\mathbf{R}-\mathbf{R}')\, d\mathbf{R}\, d\mathbf{R}'. \tag{2}$$

This is related to the average amplitude Green function $\hat{G}$ and self-energy $\hat{\Sigma}$ (in operator form) via

$$\begin{aligned} \hat{G} \equiv \langle \hat{\mathcal{G}} \rangle &= \hat{G}_0 + \hat{G}_0 \hat{T} \hat{G}_0 \\ &= \hat{G}_0 + \hat{G}_0 \hat{\Sigma} \hat{G} = [\hat{G}_0^{-1} - \hat{\Sigma}]^{-1}, \end{aligned} \tag{3}$$

$\hat{G}_0$ being the host Green function. Dependence of all these quantities on the host wave number k is implicit. The scattering path operator $\hat{\mathcal{T}}_{\alpha\beta}$ acts on the wave incident at scatterer β (located at $\mathbf{R}_\beta$) and provides the wave scattered from scatterer α, incorporating all intermediate (multiple) scattering. It may be expanded as a series in single-scatterer T matrices $\hat{t}_\alpha \equiv \hat{t}(\mathbf{R}_\alpha)$,

$$\hat{\mathcal{T}}_{\alpha\beta} = \hat{t}_\alpha \delta_{\alpha\beta} + (1-\delta_{\alpha\beta})\hat{t}_\alpha \hat{G}_0 \hat{t}_\beta + \sum_{\substack{\gamma\neq\alpha \\ \gamma\neq\beta}} \hat{t}_\alpha \hat{G}_0 \hat{t}_\gamma \hat{G}_0 \hat{t}_\beta + \cdots. \tag{4}$$

Following I we write

$$\begin{aligned} \hat{\tau}(\mathbf{R}-\mathbf{R}') = \rho \hat{t}^{(m)}(\mathbf{R})\, \delta(\mathbf{R}-\mathbf{R}') \\ + \rho \hat{t}^{(m)}(\mathbf{R}) \hat{H}(\mathbf{R}-\mathbf{R}') \rho \hat{t}^{(m)}(\mathbf{R}'), \end{aligned} \tag{5}$$

where the total propagator

$$\begin{aligned} \hat{H}(\mathbf{R}-\mathbf{R}') = \hat{C}(\mathbf{R}-\mathbf{R}') \\ + \int \hat{C}(\mathbf{R}-\mathbf{R}'') \rho \hat{t}^{(m)}(\mathbf{R}'') \hat{H}(\mathbf{R}''-\mathbf{R}')\, d\mathbf{R}''. \end{aligned} \tag{6}$$

Here $\hat{C}(\mathbf{R}-\mathbf{R}')$ is the direct (or medium) propagator, and in diagrammatic terms corresponds to a sum of strongly irreducible graphs. Formal manipulation of the multiple-scattering series yields an equation for the renormalized single-scatterer T matrix $\hat{t}^{(m)}(\mathbf{R})$ of the form

$$\hat{t}^{(m)}(\mathbf{R}) = \left[1 + \hat{t}^{(m)}(\mathbf{R}) \int \hat{H}(\mathbf{R}-\mathbf{R}') \rho \hat{t}^{(m)}(\mathbf{R}') \hat{G}_0\, d\mathbf{R}' \right] \hat{t}(\mathbf{R}). \tag{7}$$

For calculational purposes one generally expands each T matrix in a set of partial waves with an origin at the center of the scatterer. In the case of isotropic scatterers this series is truncated at the $l=0$ or s-wave term. Taken together with a condition that the scatterers should not overlap, this allows us to write Eqs. (6) and (7) as

$$H(R) = C(R) + \rho t^{(m)} \int C(|\mathbf{R}-\mathbf{R}'|) H(R')\, d\mathbf{R}', \tag{8}$$

$$t^{(m)} = \left[1 + 4\pi\rho t^{(m)2} \int_0^\infty R'^2 H(R') G^0(R')\, dR' \right] t, \tag{9}$$

with

$$G^0(R) = -\frac{e^{ik^+R}}{R} \quad (k^+ = k + i0). \tag{10}$$

Here $t \equiv t_0(k,k)$ and $t^{(m)} \equiv t_0^{(m)}(k,k)$ are the s-wave T matrices (now simply complex numbers) evaluated on shell. Notice that isotropy of the averaged system allows us to replace the vector arguments of the s-wave propagators H, C, and G^0 by their moduli.

Up to this point our analysis has been exact, apart from the assumption of isotropic scatterers. However, $C(R)$ involves an infinite series of terms, which it is not generally possible to resum. In the customary spirit of many-body theory one may hope to identify, on the strength of physical arguments, or otherwise, certain infinite subclasses of terms

which may be resummed. The remaining terms are then discarded in the hope that they do not represent a significant contribution.

Among the class of theories which may be derived in this way, the effective medium approximation is one of the most successful. In resummed form it may be summarized via the closure relation

$$C(R)=g(R)G^0(R)+h(R)[H(R)-C(R)] \quad \text{(EMA)}, \tag{11}$$

where $g(R)$ $[=h(R)+1]$ is the pair-correlation function.

Notice that in the limit of point scatterers, for which $h(R)\to 0$ for all R, $C(R)$ reduces to the bare propagator $G^0(R)$. This is a reasonable assumption, provided that the scatterers are sufficiently weak that their optical volumes do not overlap in this limit. Where this is not the case, one needs to incorporate terms which describe the renormalization of $C(R)$ via repeated scattering between pairs of scatterers. Such terms are included in the treatment of van Tiggelen *et al.* [8,12,14], which, however, expressly omits correlations. It is possible to graft pairwise correlations onto such a theory [15], and thereby study effects which accompany the onset of short-range order. However, such an approach is not readily disposed towards studying the behavior at large packing fractions. In particular, one expects significant contributions from recurrent scattering paths which involve more than two correlated scatterers. These are incorporated quite naturally in the EMA, which employs the Kirkwood decomposition [16] for higher order correlation functions.

Our principal task in this paper is to determine the wave number for the ensemble-averaged (or coherent) wave. This is found by examining the long-distance behavior of the total Green function, or equivalently from the dominant pole of the plane-wave matrix element $G(p,k)\equiv\langle \mathbf{p}|\hat{G}(k)|\mathbf{p}\rangle$. In fact, the singularities of $G(p,k)$ coincide with those of

$$H(p,k)\equiv\frac{4\pi}{p}\int_0^\infty RH(R;k)\sin pR\,dR \tag{12}$$

(the dependence on k now being made explicit). This may be seen in the following way. Since the asymptotic form of $C(R)$ coincides with that of $G^0(R)$, it is instructive to separate out $C_0(R)\equiv C(R)-G^0(R)$. Taking the Fourier transform of Eq. (8) [with $C_0(p,k)$ and $G^0(p,k)$ defined by analogy with $H(p,k)$] it now follows that

$$H(p,k)=\frac{(k^{+2}-p^2)C_0(p,k)+4\pi}{(k^{+2}-p^2)[1-\rho t^{(m)}C_0(p,k)]-4\pi\rho t^{(m)}}, \tag{13}$$

where we used the result

$$G^0(p,k)=\frac{4\pi}{k^{+2}-p^2}. \tag{14}$$

Now from Eqs. (2), (3), and (5) we have

$$G(p,k)=G^0(p,k)+G^0(p,k)[\rho t^{(m)}+\rho^2 t^{(m)2}H(p,k)]G^0(p,k), \tag{15}$$

which, on substitution of Eq. (13) yields

$$G(p,k)=\frac{1}{k^{+2}-p^2-\Sigma(p,k)}, \tag{16}$$

with the self-energy given by

$$\Sigma(p,k)=\frac{4\pi\rho t^{(m)}}{1-\rho t^{(m)}C_0(p,k)}. \tag{17}$$

In general $G(p,k)$ will have an infinite set of poles p_n, which define the real-space Green function via

$$G(R)=\sum_n A_n\frac{e^{ip_nR}}{R}, \tag{18}$$

each coefficient A_n being determined by the residue of $G(p,k)$ at p_n. The dominant pole p_0, which governs the asymptotic form of $G(R)$, has the smallest imaginary part. For small ρ we see from Eqs. (16) and (17) that it lies close to k.

The coherent wave number may also be deduced from the spectral function

$$S(p,k)=-\frac{1}{\pi}\mathrm{Im}G(p,k), \tag{19}$$

which exhibits a peak on the real p axis at $p=\mathrm{Re}(p_0)$ of half-width (at half height) $\Delta p=\mathrm{Im}(p_0)=1/(2l_s)$.

III. ANALYTICAL RESULTS FOR THE HOLE-CORRECTION APPROXIMATION

To incorporate a description of correlation effects, van Tiggelen and Lagendijk [15] made use of a simple step-function or hole-correction model, in which particles are excluded from a spherical region of radius d [21] around a given particle. Beyond this distance the distribution of other particles is assumed uniform.

Adopting this model, we now demonstrate the possibility of an analytical solution to the multiple-scattering EMA. Winn and Logan [22] obtained a similar result for a tight-binding model, from which the present solution may be recovered by analytic continuation.

We first note that Eq. (8) for the total Green function $H(R)$ has the same form as the OZ equation of a simple one-component fluid. The only difference is that the number density is now multiplied by the complex quantity $t^{(m)}$, which is determined self-consistently via Eq. (9).

Now, in the case of the EMA, we may further exploit the liquid-state analogy if we adopt the simple step-function or HC form

$$g(R)=\begin{cases}0 & \text{for } R<d\\ 1 & \text{for } R>d,\end{cases} \tag{20}$$

for the pair-correlation function. Equation (11) then becomes

$$H(R)=0 \quad \text{for } R<d, \tag{21a}$$

$$C(R)=G^0(R) \quad \text{for } R>d. \tag{21b}$$

This bears a close resemblance to the mean-spherical approximation (MSA) of liquid-state theory [16], for which

$$h(R)=0 \quad \text{for } R<d, \tag{22a}$$

$$c(R)=-\beta\phi(R) \quad \text{for } R>d, \tag{22b}$$

with $\phi(R)$ the particle-particle pair potential. Here $\beta=(k_BT)^{-1}$, T being the temperature and k_B Boltzmann's constant. In the present context $\beta\phi(R)$ is clearly replaced by $\exp(ik^+R)/R$, which corresponds to a hard-sphere fluid with a (complex) Yukawa potential. Since the Yukawa problem has been solved elsewhere [23], one may hope that a solution to the present problem may be inferred by analytic continuation. This may be confirmed via a more rigorous derivation, using the Wiener-Hopf method [20]. We give here a brief résumé of the necessary arguments.

From Eq. (13) we may write (with k dependence understood)

$$1+\rho t^{(m)}H(p)=[A(p)]^{-1}, \tag{23}$$

where

$$A(p)=1-\rho t^{(m)}\left[C_0(p)+\frac{4\pi}{k^{+2}-p^2}\right]. \tag{24}$$

Since we are dealing with a disordered system, we expect the coherent wave amplitude to decay with distance. Hence, $RH(R)\to 0$ as $R\to\infty$, and the left hand side of Eq. (23) is finite. This implies that $A(p)$ is free from zeros on the real p axis. The Wiener-Hopf argument usually proceeds by showing that $A(p)$ can be factored as

$$A(p)=Q(p)Q(-p). \tag{25}$$

In the present case this relies on the fact that k^+ has a vanishingly small (positive) imaginary part, which shifts the poles of $A(p)$ off the real p axis. We may then show that $1-Q(p)$ is Fourier transformable, allowing us to define $Q(R)$ via

$$2\pi t^{(m)}Q(R)=\frac{1}{2\pi}\int_{-\infty}^{\infty}e^{-ipR}[1-Q(p)]dp. \tag{26}$$

It also follows that

$$Q(R)=\begin{cases}0 & \text{for } R<0,\\ Q_0(R)+De^{ik^+R} & \text{for } R>0,\end{cases} \tag{27}$$

where $Q_0(R)$ vanishes for $R>d$, and D is determined by demanding continuity of $Q(R)$ at $R=d$.

The original problem may now be reexpressed in terms of two one-dimensional integral equations,

$$RC(R)=-Q'(R)+2\pi\rho t^{(m)}\int_R^{\infty}Q(R'-R)Q'(R')dR', \tag{28a}$$

$$RH(R)=-Q'(R)+2\pi\rho t^{(m)}\int_0^{\infty}Q(R')(R-R')H(|R-R'|)dR', \tag{28b}$$

the primes on Q denoting derivatives. Solution of these is achieved by exploiting the closure relation (21). After some straightforward but rather lengthy manipulation we arrive at

$$RC_0(R)=\begin{cases}2\tilde{\sigma}+(1-2\tilde{\sigma})e^{ik^+R} & \\ \quad +2\tilde{\sigma}^2(\cos k^+R-1) & \text{for } R<d\\ 0 & \text{for } R>d,\end{cases} \tag{29}$$

where $\tilde{\sigma}$ is related to the renormalized T matrix via

$$t^{(m)}=t[1-2ik\tilde{\sigma}t]^{-1}, \tag{30}$$

and may be shown to satisfy

$$\frac{6\eta}{(k^+d)^3}[2\tilde{\sigma}^2(\cos k^+d-1)-2\tilde{\sigma}(e^{ik^+d}-1)+e^{ik^+d}]^2 -\tilde{\sigma}(1-\tilde{\sigma})[2i\tilde{\sigma}-(kt)^{-1}]=0. \tag{31}$$

Clearly we must choose which of the possible solutions of Eq. (31) is appropriate. For $\eta=0$ there are three finite solutions, of which only $\tilde{\sigma}=0$ and 1 yield finite $t^{(m)}$. Of these, only $\tilde{\sigma}=0$ reproduces the correct single-scattering limit, $t^{(m)}=t$, and gives a positive spectral function. For $\eta>0$ we select the solution which develops continuously from this.

The point-scatterer model studied by van Tiggelen and co-workers [8,12–14] may be described by the bare s-wave T matrix

$$t=\frac{-1}{k(\Delta-i)}. \tag{32}$$

It follows that the scattering efficiency is

$$Q_s=\frac{16}{(kd)^2[\Delta^2+1]}, \tag{33}$$

there being a resonance at $\Delta=0$, with $\Delta>0$ (<0) corresponding to frequencies below (above) this.

Clearly we may adjust the resonant value of Q_s to something appropriate for describing a dielectric scatterer by varying kd. To begin with, let us consider the resonant case $\Delta=0$, and take $kd=1.5$, which gives $Q_s\approx 7.1$.

van Tiggelen *et al.* [8,12,14] introduced the dimensionless parameter

$$\tilde{\eta}\equiv\frac{4\pi\rho}{k^3} \tag{34}$$

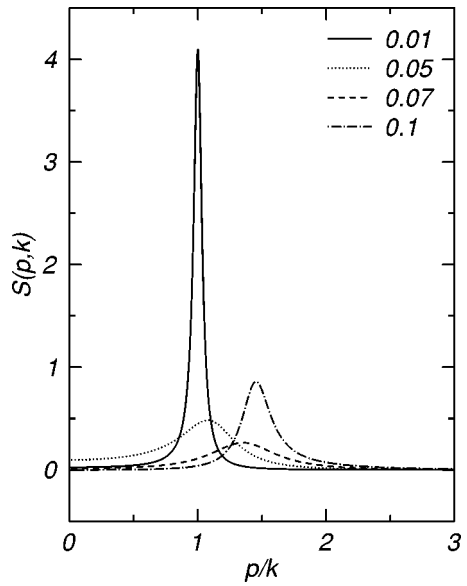

FIG. 1. Spectral function within the HC approximation for $kd=1.5$ and $\Delta=0$. The key indicates the value of packing fraction η.

[here we use the tilde to distinguish this from the packing fraction η, to which it is related via $\tilde{\eta}=24\eta/(kd)^3$]. They considered $\tilde{\eta}$ in the range 0–2, which for the above choice of kd corresponds to packing fractions up to 0.34. With the HC model we are restricted to $\eta\leqslant 1/8$, beyond which the step function $g(R)$ is no longer physically attainable for spheres of uniform size. Larger packing fractions will be investigated in Sec. IV.

Figure 1 shows the spectral function at a number of packing fractions. We see a pronounced broadening of the spectral width which appears to be largest around $\eta\approx 0.07$. This is reflected in the behavior of the coherent wave number p_0, which satisfies

$$(k^{+2}-p_0^2)[1-\rho t^{(m)}C_0(p_0,k)]-4\pi\rho t^{(m)}=0. \quad (35)$$

Figure 2 shows $n_{\rm eff}\equiv \mathrm{Re}(p_0)/k$ and $\gamma^{-1}\equiv 2\,\mathrm{Im}(p_0)/\mathrm{Re}(p_0)$, the latter being directly related to the spectral width. Pro-

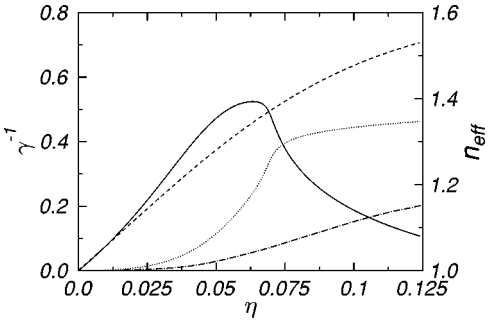

FIG. 2. Effective refractive index $n_{\rm eff}$ (dotted line) and inverse ''Ioffe-Regel'' number γ^{-1} (solid line) found by solving Eq. (35) for $kd=1.5$ and $\Delta=0$ in the HC approximation. The renormalized T matrix $t^{(m)}$ is given by Eq. (30), with $\tilde{\sigma}$ chosen as the solution of Eq. (31) which develops continuously from $\tilde{\sigma}=0$ (with increasing packing fraction η). The chained and dashed lines are the same quantities derived from the results of van Tiggelen *et al.*

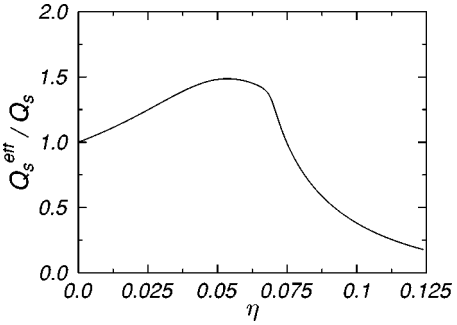

FIG. 3. Dependence of the effective scattering efficiency $Q_s^{\rm eff}$ on scatterer packing fraction η in the hole-correction EMA. The results are normalized to the single-scatterer efficiency Q_s.

vided for comparison are the analogous quantities in the theory of van Tiggelen *et al.* In plotting these we have converted their values of disorder parameter $\tilde{\eta}$ into equivalent packing fractions, having selected $kd=1.5$.

The results serve to emphasize the significant role which may be played by positional correlations. One obvious consequence is the appearance of a maximum in the EMA results for γ^{-1}. The existence of this is well established both theoretically and experimentally, and we shall not dwell on it here. We merely note that an accurate prediction of its magnitude and location demands that simultaneous account be taken of both short-range positional order and dependent scattering effects. Approaches based on either of these alone fail to capture the essential interplay.

The feature on which we focus attention is the upward curvature of γ^{-1} at small η. For independent scatterers, we would expect a linear increase with η. The observed behavior corresponds to an enhancement of the effective scattering efficiency, $Q_s^{\rm eff}$, over that for independent scatterers, as may be seen from Fig. 3. This differs from the established folklore which argues that dependent scattering reduces $Q_s^{\rm eff}$ below the single-scatterer value. The effect appears to be a direct consequence of the development of positional correlations in the system, and it is natural to ask whether one might be able to tailor this short-range order in such a way as to reach a localization threshold. This falls in line with the view [24] that one of the most promising scenarios for localization is where both Mie and Bragg-like (i.e., structural) resonances play a role.

We have observed similar behavior in other multiple-scattering calculations, involving more realistic scatterer models [25]. Behavior of this kind was also observed some time ago in experimental work on the transmission of light through TiO_2-based pigment dispersions [26], though at the time its origin was not adequately explained.

To gain a better understanding of the role of correlations we need an improved theory for $g(R)$ that is applicable at larger packing fractions. One such theory is the Percus-Yevick (PY) hard-sphere approximation to which we now turn.

IV. INCORPORATING MORE REALISTIC CORRELATION FUNCTIONS

To study the effects of a more realistic $g(R)$ it is tempting to contemplate using the asymptotic series

$$g(R)=1+\sum_{n=1}^{\infty} a_n \frac{e^{i\alpha_n R}}{R}, \tag{36}$$

truncated at some finite n, and substituting this in Eq. (11) to yield an approximate closure relation. Unfortunately the additional factor of R^{-1} that this introduces gives rise to a branch cut in $Q(p)$, which precludes use of the Baxter method. Smith [27] arrived at a similar conclusion in studying the OZ equation for a fluid with a general short-ranged pair potential.

However, it is possible to make use of the Baxter method in an approximate numerical scheme. Since the correlation function $h(R)$ becomes negligibly small when R exceeds some value R_0, we may, to a good approximation, set $h(R)=0$ for $R>R_0$. From the EMA closure relation (11) we now have

$$H(R)=0 \quad \text{for } R<d, \tag{37a}$$

$$C_0(R)=0 \quad \text{for } R>R_0, \tag{37b}$$

$$g(R)C_0(R)=h(R)H(R) \quad \text{for } d\leqslant R\leqslant R_0. \tag{37c}$$

$Q(R)$ may still be written in the form (27), but now $Q_0(R)$ is nonzero in the interval $(0, R_0)$ and D is found by requiring continuity at R_0. It is no longer possible to find a solution in closed form for $C_0(R)$. Instead we may employ

$$RC_0(R)=-Q_0'(R) + 2\pi\rho t^{(m)}\int_0^{R_0-R} Q_0'(R'+R)Q(R')dR', \tag{38}$$

which may be derived from Eq. (28a). This, together with Eq. (28b) is solved numerically, by making use of Eq. (37). For a given packing fraction the PY $g(R)$ may be determined from the hard-sphere OZ equation using an algorithm due to Goodwin *et al.* [28].

An attractive feature of this method is that it provides an immediate impression (in real space) of the effects of short-range order (SRO). For example, Fig. 4 shows the form of $RC_0(R)$ obtained in this way for two different packing fractions. For $\eta=0.07$ the graph shows a direct comparison of the results corresponding to PY and HC approximations for $g(R)$. Clearly, in the former case, the presence of SRO beyond $R=d$ causes a renormalization of the medium propagator. The effect is particularly noticeable at larger η, where the presence of ''shells'' of nearest and next-nearest neighboring spheres causes oscillations in $C_0(R)$.

As we can see from Fig. 5, the net effect of these structural correlations is an enhancement of γ^{-1}. Particularly noteworthy is the extent to which the peak near $\eta=0.07$ has narrowed and increased in height. It is apparent that the details of the SRO have a marked influence on the scattering mean free path. Given the difficulties involved in establishing the correct regime for classical wave localization, any modeling exercise ought sensibly to take account of such details. In fact, examining the form of the PY $g(R)$ leads one to question whether further enhancement of the SRO might provide an even greater increase in γ^{-1}.

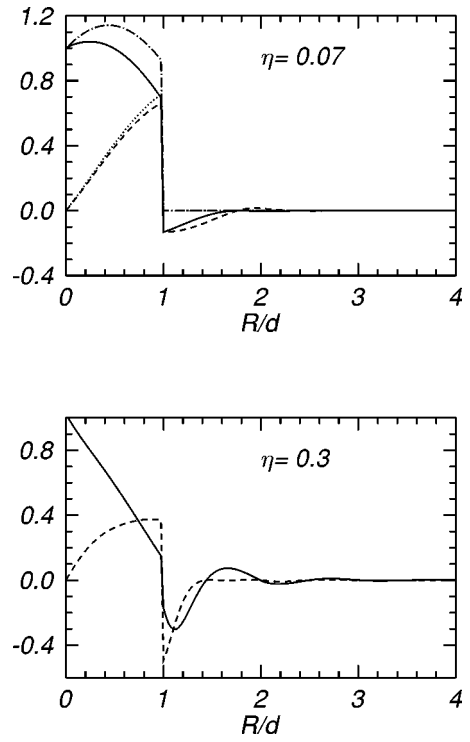

FIG. 4. EMA results for the real (solid lines) and imaginary (dashed lines) parts of $RC_0(R)$ evaluated using $kd=1.5$, $\Delta=0$, and PY correlation functions. For $\eta=0.07$ the chained and dotted lines show the corresponding quantities obtained using a HC approximation.

To this end let us consider a system of hard spheres with attractive pair potentials of the Yukawa form,

$$\phi(R)=\begin{cases} \infty & \text{for } R<d \\ -\phi_0 \dfrac{\exp(-\kappa R)}{R} & \text{for } R>d, \end{cases} \tag{39}$$

where R is the distance between the particle centers. One may think of this as a simple model potential for a monodisperse colloid. The value of κ may be adjusted to mimic the typical range of attractive pair potentials generated by adding nonadsorbing polymer to the dispersion [29]. Such a model has received some attention recently, due to its novel phase behavior [30].

For the present purposes this model is convenient, as we may employ the analytic expression for the OZ direct corre-

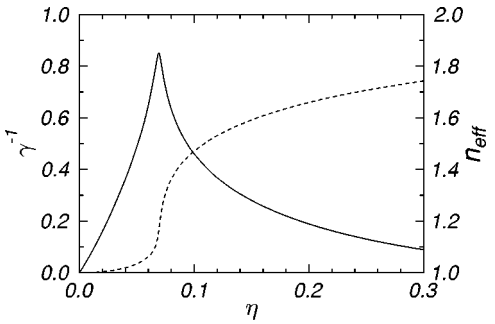

FIG. 5. γ^{-1} (solid line) and n_{eff} (dashed line) calculated in the EMA using $kd=1.5$, $\Delta=0$, and PY correlation functions.

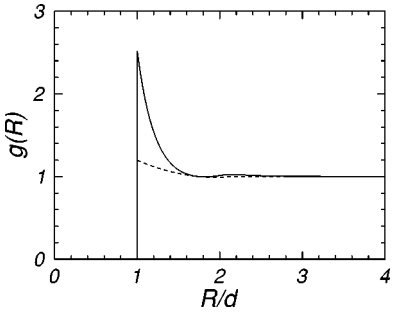

FIG. 6. Pair-correlation functions $g(R)$ at a packing fraction $\eta=0.07$. The solid line is the MSA result for Yukawa hard spheres [$\phi_0 d/(k_B T)=1.5$, $\kappa d=3.9$], and the dashed line the PY hard-sphere result.

lation function, which exists in the mean-spherical approximation [23]. Making the choice $\phi_0 d/(k_B T)=1.5$ and $\kappa d=3.9$ gives rise (for $\eta=0.07$) to the pair-correlation function shown in Fig. 6. The numerical values were found using an extension of the Goodwin *et al.* algorithm [31].

Our expectations regarding γ^{-1} appear to be borne out, judging by the results in Fig. 7. This graph provides an indication that a subtle interplay between scatterer-scatterer correlations and multiple scattering may enable a Ioffe-Regel criterion to be satisfied. Whether this coincides with the onset of localization, however, is a matter for further investigation.

It is worth remembering also, that our calculations have so far been restricted to $\Delta=0$, corresponding to the bare single-scatterer resonance. The effective scattering efficiency $Q_s^{\rm eff}$, on the other hand, generally exhibits a resonance which is shifted (in frequency) from the bare resonance. Consider Fig. 8, for example, which shows $Q_s^{\rm eff}$ as a function of Δ for a fixed ''overlap parameter'' $\tilde{\eta}=0.5$. The nature of our chosen model enables us to examine the effects of increasing the SRO by making kd larger, without the added complication of simultaneously changing the strength of the scatterers. The pronounced asymmetry of the lower two graphs, which correspond to packing fractions of 0.07 and 0.3, respectively, shows how the development of positional correlations among the scatterers can influence their collective behavior. In all cases the maximum in $Q_s^{\rm eff}$ occurs for a negative value of Δ, i.e., at a frequency above the bare resonance. Hence, as has been remarked elsewhere [14], in searching for localization it may be profitable to look at frequencies close to but not exactly at a single-scatterer resonance.

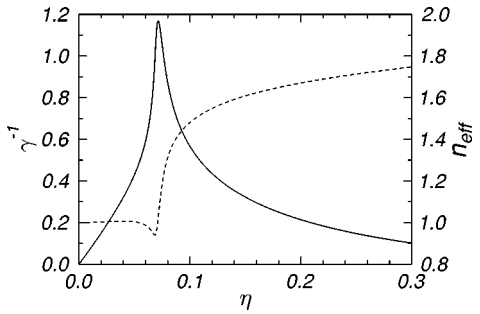

FIG. 7. As Fig. 5 but using MSA Yukawa hard sphere $g(R)$ [$\phi_0 d/(k_B T)=1.5$, $\kappa d=3.9$].

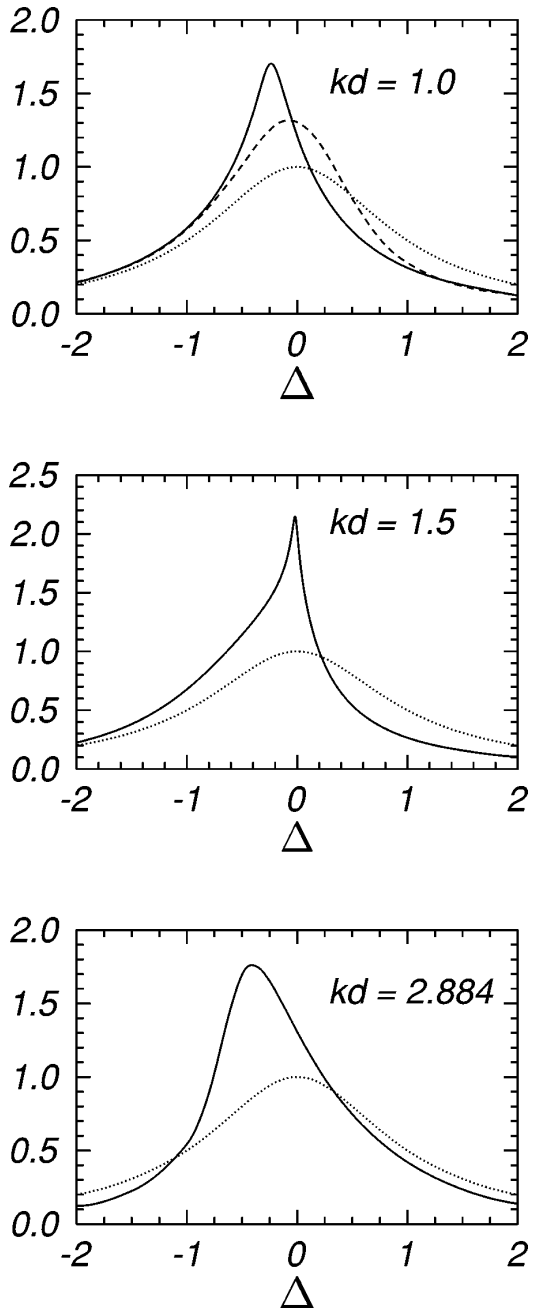

FIG. 8. EMA results (solid lines) for the effective scattering efficiency $Q_s^{\rm eff}$ as a function of Δ for $\tilde{\eta}=0.5$ and PY correlations. The dashed line for the $kd=1.0$ case derives from the work of van Tiggelen and Lagendijk [15], while the dotted lines represent the scattering efficiency Q_s of the bare single scatterer. In each graph the vertical scale is such that $Q_s=1.0$ on resonance.

We must remember, however, that within the EMA renormalization of the direct propagator is reliant on the presence of correlations. While this mechanism may be the dominant one at high packing fractions, it is not clear at what value of η other processes begin to play a role. In particular, this suggests that we exercise caution when interpreting the EMA predictions for $kd=1.0$, since they correspond to a packing fraction $\eta=0.021$.

Before concluding this section, we note that a number of other (Fourier space) schemes exist for solving the EMA [32–34]. The results reported here have been cross-checked

using an adaptation of the method of Frésard *et al.* [34] which includes a prescription for avoiding possible problems with nearly singular integrals. Following other reported experience in solving the EMA [33] Broyden's quasi-Newton algorithm [35] was employed to assist with convergence.

V. CONCLUSIONS

The influence of SRO on a system of resonant isotropic scatterers has been investigated within the EMA. Specifically, by exploiting the OZ analogy, we have shown that an analytic expression for the coherent wave dispersion relation (35) may be found in the case of correlations modeled by a HC $g(R)$. The derivation of this proceeds along the same lines as the study of a tight-binding model of a disordered conductor by Winn and Logan [22]. The extension of this approach to provide numerical results for more realistic forms of $g(R)$ has been explored and shown to be straightforward.

The results suggest a sensitive dependence of the effective scattering cross section on the details of the SRO. In these calculations we have deliberately considered only s-wave scatterers, in order to make contact with the work of van Tiggelen and Lagendijk [15]. Clearly, recurrent scattering terms of the kind they incorporate are not included in the EMA, and, in keeping with the comments of the preceding section, it is natural to ask whether these might overshadow the effects of SRO. As Winn and Logan [22] have emphasized in connection with the metal-insulator transition, such terms must be present if one is to reproduce the correct low-density behavior. This is important in the electronic context where one has a tight-binding picture and localization is expected to occur in that regime. They proposed an extension to the EMA, based on the theory of Elyutin [36]. Rewritten in a multiple-scattering language it may be summarized by the closure relation,

$$H(R)=\frac{g(R)G^{0}(R)}{1-t^{(m)2}G^{02}(R)}+g(R)[H(R)-C(R)]. \quad (40)$$

The first term on the right hand side describes recurrent scattering between pairs of scatterers. While this differs in form from the theory of van Tiggelen and Lagendijk [15], it is important to realize that, within the *exact* OZ formalism, this is the simplest theory to incorporate recurrent scattering and SRO on an equal footing.

As may be seen from Eq. (8), $H(R)-C(R)$ depends explicitly on ρ, so that the recurrent scattering term represents the dominant contribution at low density. We are currently investigating the effects of such a term. However, in contrast with electronic systems, where a metal-insulator transition obtains when $\rho\rightarrow 0$, we do not expect this limit to be important for classical wave localization due to the absence of bound ''atomic'' states. In the electronic language, a localized state must be formed by the constructive interference of scattering states. In fact, as John [24] has pointed out, we must consider frequencies which, by analogy with the Schrödinger equation, correspond to energies above the highest potential barrier. It is likely that we will need to turn the presence of correlations to our advantage by carefully tailoring the size and interactions between the scatterers.

ACKNOWLEDGMENTS

The author wishes to thank Professor T. J. Sluckin for helpful discussions, and for providing the original motivation for studying this and related problems. The work leading to this paper was supported by the EPSRC under Grants No. GR/H32124 and No. GR/K36287.

[1] *Scattering and Localization of Classical Waves in Random Media*, edited by P. Sheng (World Scientific, Singapore, 1990).
[2] *Photonic Band Gaps and Localization*, Vol. 308 of *NATO Advanced Study Institute Series B: Physics*, edited by C. M. Soukoulis (Plenum, New York, 1993).
[3] P. Sheng, *Introduction to Wave Scattering, Localization, and Mesoscopic Phenomena* (Academic, San Diego, 1995).
[4] P. A. Lee and T. V. Ramakrishnan, Rev. Mod. Phys. **57**, 287 (1985).
[5] B. Kramer and A. MacKinnon, Rep. Prog. Phys. **57**, 287 (1993).
[6] L. L. Foldy, Phys. Rev. **67**, 107 (1945).
[7] A. F. Ioffe and A. R. Regel, Prog. Semicond. **4**, 237 (1960).
[8] B. A. van Tiggelen, A. Lagendijk, and A. Tip, J. Phys.: Condens. Matter **2**, 7653 (1990).
[9] M. P. van Albada, M. B. van der Mark, and A. Lagendijk, in *Scattering and Localization of Classical Waves in Random Media*, Ref. [1].
[10] P. M. Saulnier, M. P. Zinkin, and G. H. Watson, Phys. Rev. B **42**, 2621 (1990); see also G. H. Watson, P. M. Saulnier, I. I. Tarhan, and M. P. Zinkin, in *Photonic Band Gaps and Localization*, Ref. [2].
[11] M. B. van der Mark, M. P. van Albada, and A. Lagendijk, Phys. Rev. B **37**, 3575 (1988).
[12] B. A. van Tiggelen, A. Lagendijk, A. J. Tip, and G. F. Reiter, Europhys. Lett. **15**, 535 (1991).
[13] Th. M. Nieuwenhuizen, A. Lagendijk, and B. A. van Tiggelen, Phys. Lett. A **169**, 191 (1992).
[14] B. A. van Tiggelen, Ph.D. thesis, University of Amsterdam, 1992.
[15] B. A. van Tiggelen and A. Lagendijk, Phys. Rev. B **50**, 16729 (1994).
[16] J.-P. Hansen and I.-R. McDonald, *Theory of Simple Liquids*, 2nd ed. (Academic, London, 1986).
[17] M. Lax, Rev. Mod. Phys. **23**, 287 (1951); Phys. Rev. **85**, 621 (1952).
[18] L. M. Roth, Phys. Rev. B **22**, 2793 (1980).
[19] C. J. Walden, Phys. Rev. E **52**, 3115 (1995).
[20] R. J. Baxter, Aust. J. Phys. **21**, 563 (1968).
[21] Note that the radius a to which they refer is that of the excluded region, and not that of the scatterer itself. Also, for $E_0a=2.0$ the step function $g(R)$ is not physically attainable due to a lack of available volume.
[22] M. D. Winn and D. E. Logan, J. Phys.: Condens. Matter **1**, 1753 (1988).

[23] E. Waisman, Mol. Phys. **25**, 45 (1973).
[24] S. John, in *Scattering and Localization of Classical Waves in Random Media*, Ref. [1]; also in *Photonic Band Gaps and Localization*, Ref. [2].
[25] C. J. Walden *et al.* (unpublished).
[26] W. Hughes, R. D. Murley, and D. F. Tunstall (unpublished).
[27] E. R. Smith, Mol. Phys. **38**, 823 (1979).
[28] S. P. Goodwin, J. D. Boughey, and J. R. Heritage, Mol. Phys. **75**, 917 (1992).
[29] E. J. Meijer and D. Frenkel, Phys. Rev. Lett. **67**, 1110 (1991).
[30] M. H. J. Hagen and D. Frenkel, J. Chem. Phys. **101**, 4093 (1994).
[31] C. J. Walden (unpublished).
[32] L. Huisman, D. Nicholson, L. Schwartz, and A. Bansil, Phys. Rev. B **24**, 1824 (1981).
[33] V. A. Singh and P. Bendt, Phys. Rev. B **27**, 6464 (1983).
[34] R. Frésard, H. Beck, and M. Itoh, J. Phys.: Condens. Matter **2**, 8827 (1990).
[35] See, e.g., *Numerical Recipes: The Art of Scientific Computing*, 2nd ed., edited by W. H. Press, S. A. Teukolsky, W. T. Vetterling, and B. P. Flannery (Cambridge University Press, Cambridge, England, 1992).
[36] P. V. Elyutin, J. Phys. C **14**, 1435 (1981).